
















RESEARCH ARTICLE | JUNE 06 2024

## LIBS diagnostics of Be-based samples with different gas impurities

Special Collection: [Proceedings of PLASMA 2023 - International Conference on Research and Applications of Plasmas](#)

M. Ladygina ; W. Gromelski ; P. Gasior ; A. Marín Roldán ; J. Karhunen ; P. Paris ; I. Jögi ; A. Hakola ; J. Likonen ; S. Almaviva ; J. Ristkok ; P. G. Bhat ; C. Porosnicu ; C. Lungu ; P. Veis 



*Phys. Plasmas* 31, 063501 (2024)

<https://doi.org/10.1063/5.0205561>



### Articles You May Be Interested In

ANN based LIBS models for quasi-experimental spectra relevant for materials for next-step fusion reactors

*Phys. Plasmas* (May 2024)

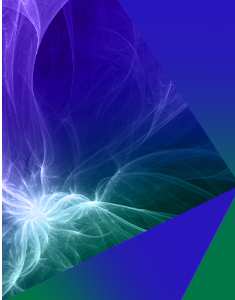
A foreword to the special issue: Proceedings of PLASMA 2023—International Conference on Research and Applications of Plasmas

*Phys. Plasmas* (April 2025)

The influence of laser energy on deuterium emission characteristics from a Zircaloy-4 plasma

*Phys. Plasmas* (October 2024)


24 June 2025 08:14:53



**Physics of Plasmas** [Learn more](#)

**Read our Author Testimonials**

*Physics of Plasmas* has a **9.1** author satisfaction rating



# LIBS diagnostics of Be-based samples with different gas impurities

Cite as: Phys. Plasmas **31**, 063501 (2024); doi: 10.1063/5.0205561

Submitted: 27 February 2024 · Accepted: 23 May 2024 ·

Published Online: 6 June 2024



View Online



Export Citation



CrossMark

M. Ladygina,<sup>1,2,a)</sup>  W. Gromelski,<sup>1</sup>  P. Gasior,<sup>1</sup>  A. Marín Roldán,<sup>3</sup>  J. Karhunen,<sup>4</sup>  P. Paris,<sup>5</sup>  I. Jögi,<sup>5</sup>   
A. Hakola,<sup>4</sup>  J. Likonen,<sup>4</sup>  S. Almaviva,<sup>6</sup>  J. Ristkok,<sup>5</sup>  P. G. Bhat,<sup>3</sup>  C. Porosnicu,<sup>7</sup>  C. Lungu,<sup>7</sup>   
and P. Veis<sup>3</sup> 

## AFFILIATIONS

<sup>1</sup>IPPLM Institute of Plasma Physics and Laser Microfusion, Hery Street 23, Warsaw 01-497, Poland

<sup>2</sup>National Science Center, Kharkiv Institute of Physics and Technology, Akademichna Street 1, Kharkiv 61108, Ukraine

<sup>3</sup>DEP, FMPI, Comenius University, Mlynská dolina F2, Bratislava 842 48, Slovakia

<sup>4</sup>VTT, P.O. Box 1000, Espoo 02044 VTT, Finland

<sup>5</sup>Institute of Physics, University of Tartu, W. Ostwaldi str. 1, Tartu 50411, Estonia

<sup>6</sup>ENEA, Italian National Agency for New Technologies, Energy and Sustainable Economic Development, Frascati Research Center, via Enrico Fermi, 45, Frascati I-00044, Italy

<sup>7</sup>INFLPR 409, Magurele, Jud Ilfov, Bucharest 077125, Romania

**Note:** This paper is part of the Special Topic, Proceedings of PLASMA 2023 - International Conference on Research and Applications of Plasmas.

<sup>a)</sup> Author to whom correspondence should be addressed: [maryna.ladygina@ifpilm.pl](mailto:maryna.ladygina@ifpilm.pl)

## ABSTRACT

Controlling plasma fuel retained in the plasma facing components of the first wall of a fusion reactor is one of the most important challenges influencing safe operation of the International Thermonuclear Experimental Reactor in the first place. This issue is proposed to be addressed by the laser-induced breakdown spectroscopy (LIBS) diagnostics, which is particularly powerful in studying the near-surface deposits and analyzing their composition. The main goal of the present study is determining the depth profiles of different elements in beryllium-based materials and the possible co-deposited layers that are formed on the walls of the Joint European Torus (JET) fusion device. Depth profiles estimated by LIBS are compared with those measured by secondary ion mass spectrometry, furthermore, the differences are discussed. In particular, the evolution of spectral lines of Be, as well as the main gaseous elements, such as Ne, N, O, and D, incorporated into the samples were extracted at different depths in the layers. LIBS diagnostics allowed making a fairly accurate analysis of the detected spectral lines of the elements on the samples. The effect of variations of the ablation rate and uncertainty that it introduces in LIBS measurements was also discussed. This investigation will have a significant impact on the development of pre-processing algorithms for machine learning models in terms of adaptation models operating on synthetic data for processing experimental spectra and is important from a point of view of LIBS tests being under preparation at JET.

© 2024 Author(s). All article content, except where otherwise noted, is licensed under a Creative Commons Attribution (CC BY) license (<https://creativecommons.org/licenses/by/4.0/>). <https://doi.org/10.1063/5.0205561>

## I. INTRODUCTION

Determining fuel retention and impurity contents of layers deposited in different areas of fusion reactors are necessary for both safety and operational reasons. The beryllium main wall in the Joint European Torus (JET) fusion reactor helps to reduce the radiation losses from the plasma and acts as an oxygen impurities getter.<sup>1,2</sup> Nevertheless, during fusion reactor experiments, the buildup of

Be-containing co-deposits with the plasma fuel can lead to unsafe operating conditions, particularly due to the increased retention of radioactive tritium.<sup>3</sup> To maintain reactor purity and achieve optimal performance, stringent control over the location, composition, and thickness of deposited layers is essential.<sup>4</sup>

In laser-induced breakdown spectroscopy (LIBS), a laser pulse ablates material from a surface, creating a plasma plume. The spectral

analysis of the optical emission from the plasma plume provides valuable information on the composition of the surface layers. By sequentially ablating and analyzing the surface, LIBS enables depth-resolved studies of the material with a resolution of a few tens up to several hundreds of nanometers, depending primarily on not only the laser fluence but also on the material properties and the structure of the layers.<sup>5</sup>

LIBS is one of the few *in situ* methods available for such depth profile investigations for fusion related samples. Moreover, LIBS together with a calibration free (CF) approach can provide depth profiling together with quantitative elemental composition analysis,<sup>6,7</sup> LIBS can be applied on a remote handling system to identify the location of co-deposits in the vacuum chamber as well as fuel retention content, which is required for nuclear safety and the estimation of the tritium inventory. Moreover, the effectiveness of fuel removal activities can be assessed by the LIBS system by application after wall cleaning. The quantification of fuel release from W, Be, and their deposits and the technological aspects of a remote handling application inside a vessel with tungsten first wall and neutrons are the main directions of LIBS applications.<sup>8–10</sup>

One of the disadvantages of LIBS methods is the matrix effect which means that the intensity of the LIBS signal depends on the chemical and mechanical properties of the investigated material. The laser ablation rate is also sensitive to the matrix effect and, therefore, the applied LIBS shot numbers are not directly related to the thickness of the ablated material. The ablation of material also means that LIBS is a destructive method even though the impact remains local. There are also other analysis methods that are suitable for the composition and hydrogen isotope retention measurements, such as secondary ion mass spectrometry (SIMS), proton induced x-ray emission (PIXE), nuclear reaction analysis (NRA), and time-of-flight elastic recoil detection analysis (ToF-ERDA).<sup>11</sup> SIMS has better depth resolution and is less sensitive to matrix effects when compared to LIBS, but it is a semi-quantitative method,<sup>5,7,12–14</sup> and destructive, similar to LIBS. PIXE allows precise quantification of elemental concentrations and is non-destructive but is only useful for elements heavier than sodium,<sup>11,13,15</sup> NRA is a nondestructive method that has high sensitivity for isotopes, such as deuterium, and it can give both depth distribution and total retention<sup>13,15–17</sup> in a few micrometers thick layer; however, reconstructing accurate depth profiles is challenging. ToF-ERDA is non-destructive and useful for quantitative depth profiling of all isotopes but is limited to thicknesses below one micrometer,<sup>18,19</sup> However, these methods are not suitable for *in situ* studies.

In the present study, LIBS was applied to a number of reference samples with different compositions imitating/resembling co-deposits with hydrogen isotopes, He ash, and seeding gases, Ne or N. Such coatings are relevant for upcoming test experiments at JET and advantageous from the point of view of the development machine learning (ML) algorithms for LIBS. The ML algorithm,<sup>20</sup> especially the deep neural networks foreseen for this investigation trained on a considerable amount of experimental data, will be capable of providing compensation for numerous effects affecting the accuracy of CF-LIBS, such as operation conditions, sample porosity changing the ablation rate, and hence the evaluation of the critical plasma parameters like the electron temperature  $T_e$ .

## II. EXPERIMENTAL SETUP, DIAGNOSTICS, AND SAMPLES

The studies were carried out using the experimental setup for LIBS studies of beryllium-containing samples located in VTT

(Technical Research Center of Finland Ltd.),<sup>21</sup> the scheme is presented in Fig. 1.

A pulsed Nd:YAG laser (Brilliant B, Quantel, 1064 nm, 5 ns) coupled with an Andor SR-750 spectrometer equipped with an Andor iStar 340T ICCD camera was used as the LIBS diagnostics. Plasma emission was collected perpendicularly to the laser beam using an off-axis parabolic mirror and guided to a fiber bundle that was connected to the entrance slit of the spectrometer. For good depth profiling, the fluence of the laser beam at the target surface of  $\sim 4.5 \text{ J/cm}^2$  was used. The size (FWHM) of the focused laser spot is approximately 1.2 mm. The emission was collected from a distance of 3, 6, or 11 mm from the target surface. The size of the plume region collected by the spectrometer was 2.5–3 mm in diameter. The resolution of the spectrometer lies in the frame of 0.01–0.03 nm depending on the wavelength range. The delay time between the laser shot and the collection of spectra by the ICCD camera and the gate width of the camera were set to 200 ns, but for the 656 nm spectral window, the delay and gate width of 4  $\mu\text{s}$  were for a clearer distinction between isotopes.

The vacuum chamber was filled with Ar gas. In the current research, the data with pressure of 2 mbar were analyzed. The depth profiles for each measurement spot were reconstructed from a kinetic series of 100 laser shots. More details about experimental conditions are described in Ref. 22.

The samples were produced with beryllium coatings, containing D, He, Ne, and N impurities with different concentrations that were deposited onto the W substrate. Those elements will be among the main ones to occur in deposited layers on the wall structures of fusion reactors, since D is used for fuel, He is the product of fusion reactions, N and Ne are typical seeding impurities into the edge plasma. All details about their production are presented in Ref. 18. The sample composition was determined by TOF-ERDA and sample thickness by SIMS method.

Figure 2 shows an example of one of the samples together with LIBS craters.

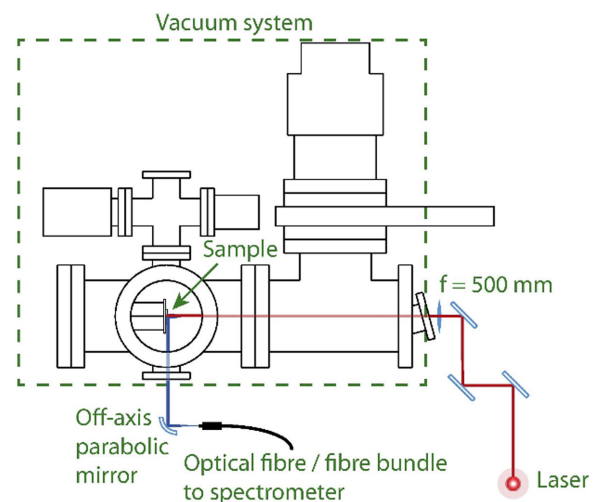
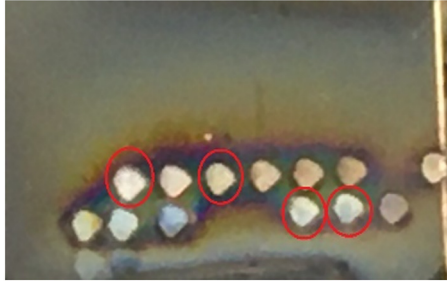


FIG. 1. The scheme of the experimental setup with LIBS diagnostics.<sup>12</sup> Reproduced with permission from Karhunen *et al.*, "Applicability of LIBS for in situ monitoring of deposition and retention on the ITER-like wall of JET – Comparison to SIMS," *J. Nucl. Mater.* **463**, 931–935 (2015). Copyright 2015 Elsevier. Reproduced with permission.



**FIG. 2.** The photo of sample Be90%D5%He5% with LIBS craters. Craters signed by red will be analyzed in Sec. III B.

The present work shows the results and analysis of the experiments performed with samples with various nominal gas-beryllium ratio content that are presented in Table I.

It should be noted that Ne spectral lines were not detected in the spectra, probably due to its small concentration and/or because of its high excitation energy. At the same time, D and He spectral lines were registered and studied in detail. Additional information related to the gas content of the samples, particularly on the H $\alpha$ /D $\alpha$  line was collected and carefully analyzed by coauthors and published in Ref. 22, whereas the studies of the He line were published separately.<sup>23</sup>

### III. RESULTS AND DISCUSSION

#### A. LIBS depth profiles of chemical components for different types of samples

Examples of the spectra that were recorded during LIBS measurements of different Be-containing samples are shown in Fig. 3. The data are taken after 1, 5, 10, and 20 laser shots, to track the dynamics of the spectral line intensities for two chosen samples in different wavelength ranges.

The depth profiles of individual elements were extracted as a function of the number of laser pulses incident on the sample.

In Fig. 4, the depth profiles of the spectral lines of Be, W, Ar, and H $\alpha$ /D $\alpha$  are presented for the above-mentioned samples, where the depth profile of the same elemental lines is noticeably different between the samples. At the same time, it should be noted that different lines within the same sample correlated with each other. Moreover, the lines were taken from different craters, and in general, show similar behavior for the same sample. The lines were normalized to their maximum intensity in the series of the applied laser pulses and smoothed for tracking of their behavior and easy comparison.

In the sample 2, Be92,5%D5%He2,5% (Fig. 4), Be is present for the first 9–10 pulses, whereas the depth profiles for the H $\alpha$ /D $\alpha$  line show narrower peaks indicating that hydrogenic isotopes are accumulated close to the surface or are desorbed from deeper layers by means of the heat transport. During the laser pulses, the intensity of the W line grows up to the 10th shot, indicating that the substrate was reached at this depth.

In sample 4, Be85%D10%Ne5%, the Be I and II intensity drops after 20–25 shots, and, respectively, the W lines' intensity starts to grow approximately from this depth.

To estimate the LIBS ablation rate of the Be layer, we assumed that the intersection of the Be and W intensity profiles (in terms of the

**TABLE I.** Title and the chemical composition of the investigated samples.

Sample number	Title of sample	TOF-ERDA (at. %)				
		Be	D	O	He	Ne
1	Be95%D5%	93	2–3	1–4	...	...
2	Be92,5%D5%He2,5%	95	~1	1	0.5	...
3	Be90%D5%He5%	89	~4	1	3	...
4	Be85%D10%Ne5%	88	5–9	1–4		<1

number of laser pulses) corresponded to the interface between the Be layer and the underlying substrate.

The vertical dotted lines in Fig. 4 indicate the approximate depth of the interface between the Be layer and the W bulk material. The thickness of the top Be layer determined by profilometry of SIMS craters is also shown on the bottom axis.

The substantial variation in the shape of depth profiles suggests a fluctuation in the ablation rate, i.e., the amount of material removed from the surface by irradiating it with a laser beam per shot may change in dependence of the layer material. The layers having the same thickness can show different ablation rates, and D inclusion typically makes the deposited layers softer.<sup>7</sup> It is worth noting that these findings may have implications for machine learning algorithms being under development, since all the uncertainties in the profiles must be taken into account when data are processed for training and/or validating the models.

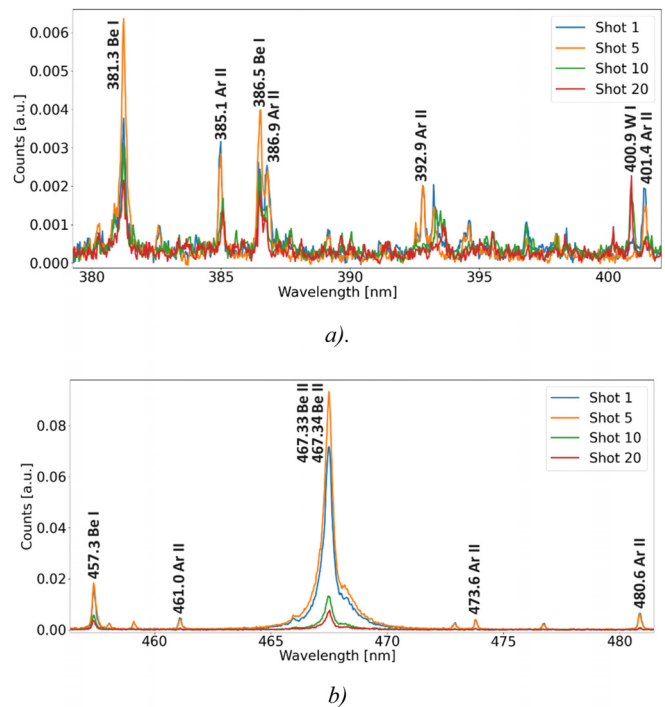
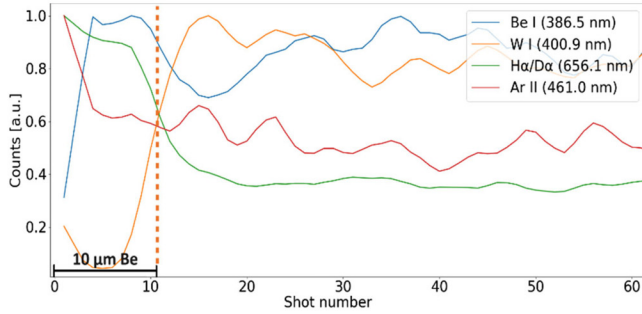


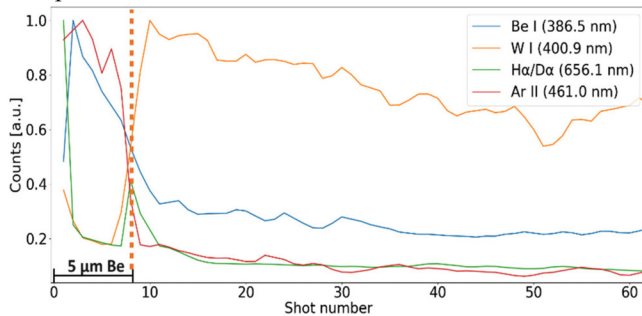
**FIG. 3.** Spectra detected with sample Be92,5%D5%He2,5% (a) 380–402 nm; (b) 455–481 nm.

The ablation rate was calculated by dividing the thickness of the sample, measured by profilometry of SIMS craters, by the number of laser pulses required to reach the Be and W interfaces (shown by vertical lines) that were taken from Fig. 4. All the necessary parameters for

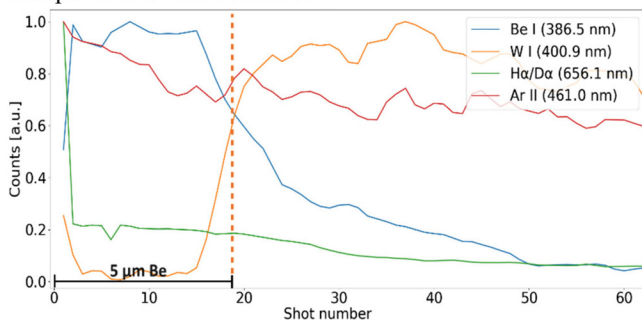
Sample 1: Be95%D5%



Sample 2: Be92.5%D5%He2.5%



Sample 3: Be90%D5%He5%



Sample 4: Be85%D10%Ne5%

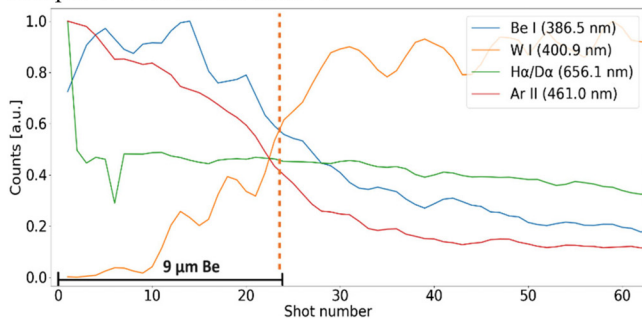


FIG. 4. LIBS depth profiles of chemical components for samples with different seed gas (D, He, and Ne) concentrations.

evaluating ablation rates are summarized in Table II. As can be seen, the ablation rate has a strong fluctuation between the different samples, which indicates differences between the properties of the coatings. The ablation rates that were obtained are averaged over the laser shots required to reach the interface, but even then, it shows remarkable differences in the values. The effect of the properties of the Be coatings on the ablation rates should be investigated further.

It is worth mentioning that additional craters and their corresponding spectral lines were also investigated. While minor deviations were observed, these differences exerted minimal influence on the overall trend of the depth profiles.

**B. Influence of the crater position on Be line profiles on the sample (Be90%D5%He5%)**

As an exception, there were a few craters in which the behavior of the depth profiles of some spectral lines was significantly different. Such craters were omitted when studying depth profiles shown in Fig. 3, since the reasons for the differences should be studied more carefully.

For this purpose, a map of the behavior of the beryllium depth profiles was constructed for one of the samples in order to clarify the issue of the uniformity of this coating over the entire surface of the sample. Figure 5(a) shows the number of craters that were available and chosen for this study and the photo of the sample with corresponding craters. The typical behavior for Be lines, which was observed in most cases, is tracked in craters 6 and 7, and in craters 15 and 17, the other atypical behavior for the current experiments is seen in Fig. 5(b). Be and W depth profiles for craters 6, 7 and 15, 17 are added below.

Relatively high variations in the depth profiles of the craters may suggest variation in the Be coating thickness, and thus, possible imperfections of the produced samples. However, the influence of other factors, such as observation parameters, cannot be excluded—the optical emission was collected closer to the target surface (3 mm) for craters 15–17 when compared to the craters 6–7 (6 mm). The variation of depth profiles corresponding to different craters was much smaller for W or Ar lines. This suggests that the LIBS depth profiles are also influenced by the collection distance.

The line of sight for recording the spectra was parallel to the sample surface.

To investigate the actual reason for this discrepancy, additional material research methods should be employed together with the influence of the contents of seeding gases, which has been preliminary addressed in Ref. 22.

TABLE II. Ablation rate calculation.

Sample number	Title of sample	SIMS thickness (μm)	Edge of coating (shot)	Ablation rate (μm/shot)
1	Be95%D5%	~10	10	1
2	Be92,5%D5%He2,5%	~5	8	0.63
3	Be90%D5%He5%	~5	19	0.26
4	Be85%D10%Ne5%	~9	23	0.39

24 June 2025 08:14:53

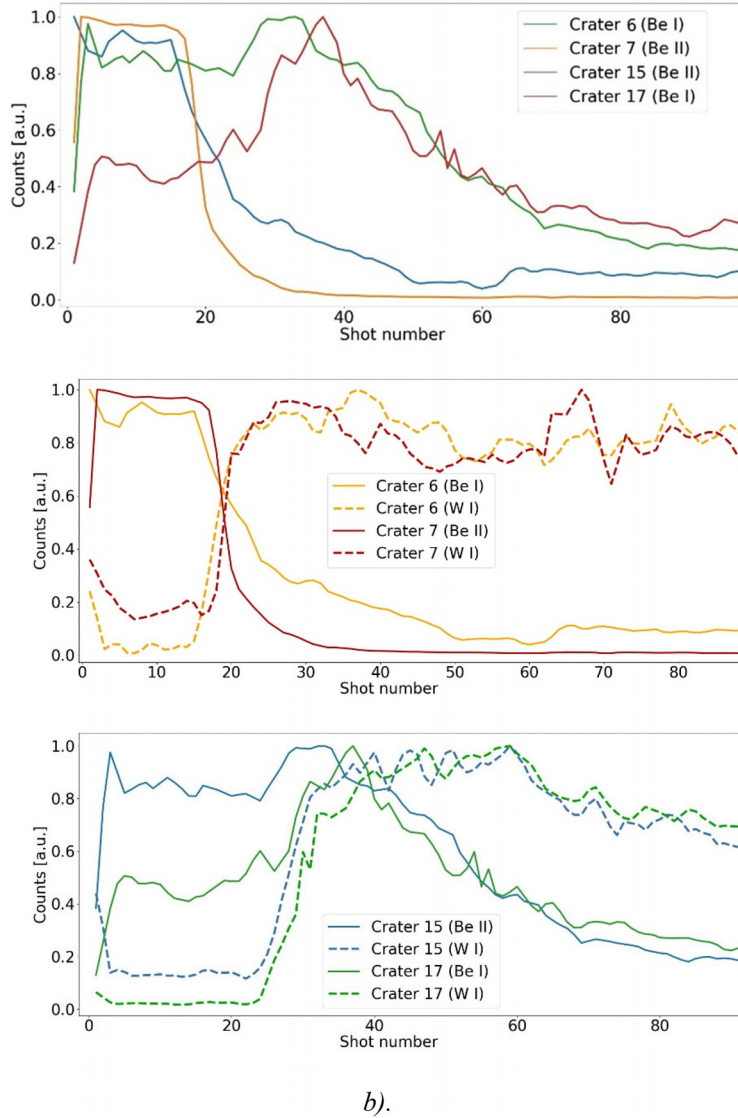
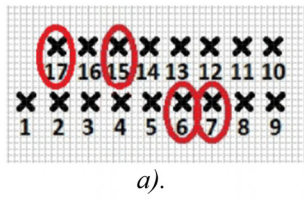


FIG. 5. (a) Map of the sample with crater numbers, corresponding to the photo (Fig. 2) and (b) depth profiles reconstructed from Be spectral lines in corresponding craters.

IV. CONCLUSIONS

The behavior of spectral lines of the components (including impurities) of JET relevant samples has been analyzed, and depth profiles are obtained.

Since the difference in coating thickness or ablation rate is visible even on the same target, it is rather difficult to draw conclusions on the effect of different Be or impurity concentrations on fuel retention obtained from other samples, which would be possible if the precision of sample production was higher. Nevertheless, LIBS diagnostics led to a fairly accurate analysis of the behavior of the detected spectral lines of the elements in the samples. However, the effect of variations in the ablation rate and the uncertainty that it introduces in LIBS measurements, which must be taken into account, should not be underestimated.

Investigation of depth profiles and their comparison with SIMS measurements will have a significant impact on the development of pre-processing algorithms for machine learning models in terms of adaptation models operating on synthetic data for processing experimental spectra. The reason for this is that pre-processing should take into account the impact of the measurement system properties on the measured spectra so that ML models operate on datasets with comparable statistical features. Moreover, one needs data with reliable information on chemical composition to validate the models, and the result of the validation is essential for the performance assessment. After pre-processing, data will be used for training ML models based on ANN, which will be the next step of work at the IPPLM.

24 June 2025 08:14:53

## ACKNOWLEDGMENTS

This scientific paper has been published as part of an international project co-financed by the Polish Ministry of Science and Higher Education within the program called “PMW” for 2023. The authors A.M.R., P.G.B., and P.V. acknowledge the Scientific Grant Agency of the Slovak Republic (Contract No. 1/0803/21) and the Slovak Research and Development Agency (APVV-22-0548) for financial support.

This work has been carried out within the framework of the EUROfusion Consortium, funded by the European Union via the Euratom Research and Training Programme (Grant Agreement No. 101052200—EUROfusion). Views and opinions expressed are, however, those of the authors only and do not necessarily reflect those of the European Union or the European Commission. Neither the European Union nor the European Commission can be held responsible for them.

The authors would like to thank all the EUROfusion PWIE contributors who were involved in this research.

## AUTHOR DECLARATIONS

## Conflict of Interest

The authors have no conflicts to disclose.

## Author Contributions

**M. Ladygina:** Conceptualization (equal); Investigation (lead); Writing – original draft (lead). **W. Gromelski:** Software (equal); Validation (equal). **P. Gasiior:** Investigation (equal); Resources (equal); Validation (equal). **A. Marín Roldán:** Resources (equal). **J. Karhunen:** Data curation (equal). **P. Paris:** Data curation (equal); Methodology (equal). **I. Jögi:** Data curation (equal); Investigation (equal); Validation (equal). **A. Hakola:** Conceptualization (equal); Data curation (equal); Validation (equal). **J. Likonen:** Resources (equal). **S. Almagiva:** Data curation (equal). **J. Ristkok:** Resources (equal). **P. G. Bhat:** Investigation (equal); Validation (equal). **C. Porosnicu:** Resources (equal). **C. Lungu:** Resources (equal). **P. Veis:** Investigation (equal); Validation (equal).

## DATA AVAILABILITY

The data that support the findings of this study are available within the article.

## REFERENCES

- <sup>1</sup>S. Brezinsek, A. Widdowson, M. Mayer, V. Philipps, P. Baron-Wiechec, J. W. Coenen, K. Heinola, A. Huber, J. Likonen, P. Petersson *et al.*, *Nucl. Fusion* **55**, 063021 (2015).
- <sup>2</sup>J. Roth, E. Tsitrona, A. Loarte, T. Loarer, G. Counsell, R. Neu, V. Philipps, S. Brezinsek, M. Lehnen, P. Coad *et al.*, *J. Nucl. Mater.* **390–391**, 1–9 (2009).
- <sup>3</sup>F. Le Guern, W. Gulden, S. Ciattaglia, G. Counsell, A. Bengaouer, J. Brinster, F. Dabbene, A. Denkevitz, T. Jordan, M. Kuznetsov *et al.*, *Fusion Eng. Des.* **86**, 2753–2757 (2011).
- <sup>4</sup>J. Mailloux, N. Abid, K. Abraham, P. Abreu, O. Adabonyan, P. Adrich, V. Afanasev, M. Afzal, T. Ahlgren, L. Aho-Mantila *et al.*, *Nucl. Fusion* **62**, 042026 (2022).
- <sup>5</sup>M. Suchoňová, P. Veis, J. Karhunen, P. Paris, M. Pribula, K. Piip, M. Laan, C. Porosnicu, C. Lungu, and A. Hakola, *Nucl. Mater. Energy* **12**, 611–616 (2017).
- <sup>6</sup>P. Veis, A. Marín-Roldán, V. Dwivedi, J. Karhunen, P. Paris, I. Jögi, C. Porosnicu, C. P. Lungu, V. Nemanic, and A. Hakola, *Phys. Scr.* **T171**, 014073 (2020).
- <sup>7</sup>V. Dwivedi, A. Marín-Roldán, J. Karhunen, P. Paris, I. Jögi, C. Porosnicu, C. P. Lungu, H. van der Meiden, A. Hakola, P. Veis *et al.*, *Nucl. Mater. Energy* **27**, 100990 (2021).
- <sup>8</sup>S. Almagiva, L. Caneve, F. Colao, V. Lazic, G. Maddaluno, P. Mosetti, A. Palucci, A. Reale, P. Gasiior, W. Gromelski *et al.*, *Fusion Eng. Des.* **157**, 111685 (2020).
- <sup>9</sup>T. L. Griffiths, S. E. Woodbury, A. Brooks, V. Pinon, A. Giakoumaki, and A. I. Whitehouse, *Spectrochim. Acta Part B* **180**, 106205 (2021).
- <sup>10</sup>H. J. van der Meiden, S. Almagiva, J. Butikova, P. Gasiior, A. Hakola, I. Jögi, G. Sergienko, P. Veis, and S. Brezinsek, *Nucl. Fusion* **61**, 125001 (2021).
- <sup>11</sup>R. Mateus, N. Catarino, M. Dias, L. C. Alves, O. Romanenko, Z. Siketić, I. Bogdanović Radović, A. Hakola, E. Grigore, E. Alves *et al.*, *Nucl. Instrum. Methods Phys. Res., Sect. B* **538**, 41–46 (2023).
- <sup>12</sup>J. Karhunen, A. Hakola, J. Likonen, A. Lissovski, M. Laan, P. Paris, and JET EFDA Contributors, “Applicability of LIBS for *in situ* monitoring of deposition and retention on the ITER-like wall of JET – Comparison to SIMS,” *J. Nucl. Mater.* **463**, 931–935 (2015).
- <sup>13</sup>K. Piip, H. J. van der Meiden, L. Hämarik, J. Karhunen, A. Hakola, M. Laan, P. Paris, M. Aints, J. Likonen, K. Bystrov *et al.*, *J. Nucl. Mater.* **489**, 129–136 (2017).
- <sup>14</sup>I. Jögi, P. Paris, M. Laan, J. Kozlova, H. Mändar, M. Passoni, D. Dellasega, A. Hakola, and H. J. van der Meiden, *J. Nucl. Mater.* **544**, 152660 (2021).
- <sup>15</sup>M. Kelemen, A. Založnik, P. Vavpetič, M. Pečovnik, P. Pelicon, A. Hakola, A. Lahtinen, J. Karhunen, K. Piip, P. Paris *et al.*, *Nucl. Instrum. Methods Phys. Res., Sect. B* **404**, 179–184 (2017).
- <sup>16</sup>P. Wang, W. Jacob, L. Gao, T. Dürbeck, and T. Schwarz-Selinger, *Nucl. Instrum. Methods Phys. Res., Sect. B* **300**, 54–61 (2013).
- <sup>17</sup>P. Paris, I. Jögi, K. Piip, M. Passoni, D. Dellasega, E. Grigore, W. M. Arnoldbik, and H. van der Meiden, *Fusion Eng. Des.* **168**, 112403 (2021).
- <sup>18</sup>A. Hakola, K. Heinola, K. Mizohata, J. Likonen, C. Lungu, C. Porosnicu, E. Alves, R. Mateus, I. B. Radovic, Z. Siketić *et al.*, *Phys. Scr.* **2020**, 014038.
- <sup>19</sup>K. Kantre, P. S. Szabo, M. V. Moro, C. Cupak, R. Stadlmayr, L. Z. Medina, F. Aumayr, and D. Primetzhofer, *Phys. Scr.* **96**, 124004 (2021).
- <sup>20</sup>P. Gasiior, W. Gromelski, M. Kastek, and A. Kwaśnik, *Spectrochim. Acta B* **199**, 106576 (2023).
- <sup>21</sup>J. Karhunen, A. Hakola, J. Likonen, A. Lissovski, P. Paris, M. Laan, K. Piip, C. Porosnicu, C. P. Lungu, and K. Sugiyamaet, *Phys. Scr.* **2014**, 014067.
- <sup>22</sup>P. G. Bhat, P. Veis, A. Marín Roldán, J. Karhunen, P. Paris, I. Jögi, A. Hakola, J. Likonen, S. Almagiva, W. Gromelski *et al.*, *Nucl. Mater. Energy* **37**, 101549 (2023).
- <sup>23</sup>I. Jögi, P. Paris, J. Ristkok, A. Marín Roldán, P. G. Bhat, P. Veis, J. Karhunen, S. Almagiva, W. Gromelski, P. Dinca *et al.*, *Nucl. Mater. Energy* **39**, 101677 (2024).